Journal of Thermal Analysis, Vol. 49 (1997) 1263-1275

DIMENSIONAL STABILITY AND DEFECT CHEMISTRY OF DOPED LANTHANUM CHROMITES

P. H. Larsen, P. V. Hendriksen and M. Mogensen

Materials Department, Risø National Laboratory, DK-4000 Roskilde, Denmark

Abstract

Acceptor doped lanthanum chromites are potential interconnect materials to be used in high temperature Solid Oxide Fuel Cells (SOFC). However, instability of these materials when exposed to low oxygen partial pressure causes a volume expansion that can be detrimental to the SOFC performance. The stability of $La_{0.8}Sr_{0.2}Cr_{0.97}V_{0.03}O_3$ is determined as function of pO_2 and temperature by isothermal thermogravimetry and dilatometry. The experimental data are analysed using a simple model for the defect chemistry. The relation between expansion behaviour and change in defect chemistry is discussed using a simple structural model.

Keywords: interconnect, isothermal expansion, SOFC

Introduction

Acceptor doped lanthanum chromites are currently being investigated as ceramic interconnector materials to be used in high temperature Solid Oxide Fuel Cells (SOFC). The interconnector provides the electrical contact between the fuel and air electrodes when single cells are stacked in series and separates the fuel and oxidant gases during operation. The requirements to such interconnects are high electronic conductivity, low ionic conductivity and thermodynamical stability in oxygen partial pressures ranging from 10^{-18} to 0.21 atm at SOFC working temperature (1000°C). Further requirements are chemical and mechanical compatibility with the other SOFC components, and the material must be sinterable to high density to ensure gas tightness [1].

The electronic conductivity of the stoichiometric $LaCrO_3$ compound (ABO_3 perovskite structure) is increased by substitution with divalent ions on either the A- or B-sites. The most frequently used dopants are Ca or Sr on the A site (Ma) or Mg on the B-site (Mb) [2–4]. The formula of such compounds can be written as $La_{1-x}Ma_xCr_{1-y}Mb_yO_{3-\delta}$, where y or x typically are in the range of 0 to 0.3, and Ma and Mb are dopants with ionic radii's compatible with the A- and B-sites respectively. The substitution of a trivalent ion with a divalent is electronically compensated by the formation of Cr(IV) ions at high pO_2, where the oxygen deficiency (δ) has been found to be close to zero [5]. At low pO_2 the compound looses oxygen to the surroundings and oxygen vacancies are formed. Charge neutrality is maintained by reduction of Cr(IV) to Cr(III) [2–5]. The change in valence state of the chromium ions and the change in oxygen vacancy concentration lead to a volume expan-

0368–4466/97/ $ 5.00

John Wiley & Sons Limited
Chichester

sion [5–8] as well as a decrease in the electronic conductivity [9, 10]. For the case of Ca-doping the mechanical strength has furthermore been found to decrease upon the reduction [11].

The difference in pO_2 between the anode and cathode compartments during operation leads to a pO_2 gradient over the interconnector plate, that causes a build up of mechanical stresses inside the interconnect plate. This may lead to mechanical damage not only to the interconnect plate, but also to the electrodes and the electrolyte [12].

The experimental part of the present study is concentrated on a composition doped with strontium on the A-site and vanadium on the B-site, $(La_{0.8}Sr_{0.2})(Cr_{0.97}V_{0.03})O_3$. The oxygen stoichiometry and the linear expansion are determined as function of pO_2 and temperature by thermogravimetry and dilatometry, respectively. The experimental data are analysed using a simple model of the defect chemistry. The equilibrium constants of the defect reactions are obtained from the TG experiments and the relation between the expansion and the changes in the defect chemistry with pO_2 are discussed.

The behaviour of the investigated material is compared to that of materials with other A- and B-site dopants reported in literature. The effect of different dopants are discussed considering the defect model and a simple structure model.

Experimental

The $(La_{0.8}Sr_{0.2})(Cr_{0.97}V_{0.03})O_3$ compounds was synthesised by the glycine method [13]. The principal cause for addition of vanadium was to improve the sinterability of the material [14]. After synthesis the powder was calcined at 1000°C, pressed and sintered at 1450°C for 2 h. Phase purity analysis with XRD showed a single phase perovskite structure.

Both dilatometry and TG analyses were performed as a function of pO_2 using a $CO_2/N_2/H_2$ system with flow rates around 300 ml min^{-1}. The pO_2 was continuously monitored by passing the exit gases to a calibrated oxygen sensor. The isothermal expansion measurements were performed using a Setaram DHT 2050 differential dilatometer on 18 mm×4 mm×6 mm bars. The samples were heated to the temperature of measurement (800, 900, 1000 or 1100°C) and allowed to equilibrate in air. After equilibrium was reached the gas composition was changed in a number of steps going from pO_2 ~10^{-5} to 10^{-20} atm and back (1000°C). The changes were monitored continuously. Equilibrium was assumed when the rate of change was less than 10^{-4} %/min.

Determinations of mass losses were performed by isothermal thermogravimetry as a function of pO_2 at temperatures 800, 900 and 1000°C. The balance used was a SEIKO TG/DTA320. Sintered samples of 200 mg were heated to the analysis temperature in air and allowed to equilibrate before each change in pO_2. The obtained data were corrected for buoyancy effects.

Theory

The defect chemistry of acceptor doped lanthanum chromite has been treated by Khattak and Cox [5] and Mizusaki *et al.* [2] for the case of Sr-doping, and by

Table 1 Ionic radii for Mg, Cr and V in 6 fold coordination with different valences and for 12 fold coordinated La and Sr [20]

	(II)	(III)	(IV)
Cr		0.615	0.55
V		0.64	0.58
Mg	0.72		
Sr	1.44		
La		1.36	

Yasuda *et al.* [10] and Flandermeyer *et al.* [4] for the cases of Ca- and Mg-doping, respectively. At high pO_2 the divalent doping is electronically compensated by formation of Cr(IV). At low pO_2 the material looses oxygen to the environment, and to maintain charge neutrality the loss of oxygen is accompanied by reduction of Cr(IV) to Cr(III). Here we consider a material doped with both Sr and V. From the ionic size of vanadium it is expected that it enters on the B-site in the perovskite structure (Table 1), and that it may be either tetravalent or trivalent. At high pO_2 the vanadium is expected to be tetravalent. At low pO_2 the vanadium may, like the chromium, be reduced to the trivalent state upon the introduction of oxygen vacancies. Using the Kröger-Vink notation the reactions of oxygen vacancy formation can be written:

$$2\mathrm{Cr}^{\cdot}_{\mathrm{Cr}} + \mathrm{O}^{\mathrm{x}}_{\mathrm{o}} \leftrightarrow 2\mathrm{Cr}^{\mathrm{x}}_{\mathrm{Cr}} + V^{\cdot\cdot}_{\mathrm{o}} + \frac{1}{2}\mathrm{O}_2\ (g) \qquad (1)$$

$$2\mathrm{V}^{\cdot}_{\mathrm{Cr}} + \mathrm{O}^{\mathrm{x}}_{\mathrm{o}} \leftrightarrow 2\mathrm{V}^{\mathrm{x}}_{\mathrm{Cr}} + V^{\cdot\cdot}_{\mathrm{o}} + \frac{1}{2}\mathrm{O}_2\ (g) \qquad (2)$$

Where $V^{\cdot\cdot}_{\mathrm{o}}$ is an oxygen vacancy and $\mathrm{V}^{\cdot}_{\mathrm{Cr}}$ and $\mathrm{V}^{\mathrm{x}}_{\mathrm{Cr}}$ are tetra- and trivalent vanadium on the chromium site, respectively (likewise for the chromium). Assuming ideal behaviour the defect concentrations are at equilibrium related to the pO_2 according to:

$$K_1 = pO_2^{1/2}\frac{[\mathrm{Cr}^{\mathrm{x}}_{\mathrm{Cr}}]^2[V^{\cdot\cdot}_{\mathrm{o}}]}{[\mathrm{Cr}^{\cdot}_{\mathrm{Cr}}]^2[\mathrm{O}^{\mathrm{x}}_{\mathrm{o}}]}, \qquad (3)$$

$$K_2 = pO_2^{1/2}\frac{[\mathrm{V}^{\mathrm{x}}_{\mathrm{Cr}}]^2[V^{\cdot\cdot}_{\mathrm{o}}]}{[\mathrm{V}^{\cdot}_{\mathrm{Cr}}]^2[\mathrm{O}^{\mathrm{x}}_{\mathrm{o}}]}, \qquad (4)$$

where K_1 and K_2 are the equilibrium constants of reactions (1) and (2), respectively. The B-site and oxygen site balances require that:

$$[\mathrm{Cr}^{\mathrm{x}}_{\mathrm{Cr}}] + [\mathrm{Cr}^{\cdot}_{\mathrm{Cr}}] = 1 - y \qquad (5)$$

$$[V^{x}_{Cr}] + [V^{\cdot}_{Cr}] = y \tag{6}$$

$$[O^{x}_{o}] = 3 - \delta \tag{7}$$

The requirement of overall charge neutrality can, under the assumption of an A/B-site ratio of one, be expressed as:

$$[V^{\cdot}_{Cr}] + [Cr^{\cdot}_{Cr}] = [Sr'_{La}] - 2[V^{\cdot\cdot}_{o}] = x - 2\delta \tag{8}$$

If the equilibrium constants K_1 and K_2 are known the oxide ion vacancy concentration and all other defect concentrations may be found at a given pO_2 by simultaneous solution of Eqs (3–8).

In the pure oxides V(IV) is much more stable than Cr(IV). The electrode potentials of the reactions

$$2CrO_2 \leftrightarrow Cr_2O_3 + 1/2O_2 \tag{9}$$

$$2VO_2 \leftrightarrow V_2O_3 + 1/2O_2 \tag{10}$$

are at 1000°C, respectively, 20 and –610 mV measured against oxygen at 1 atm. This corresponds to oxygen partial pressures of 2 atm and 10^{-10} atm, respectively. It should be noted that the value for CrO_2 is extrapolated from 600 K. Assuming that the Cr(IV) and V(IV) are stabilized similarly in the perovskite lattice in $(La_{0.8}Sr_{0.2})(Cr_{0.97}V_{0.03})O_3$ the reduction of Cr(IV) is expected to occur at much higher pO_2, than the reduction of V(IV). In the following it is thus assumed that $[V^{\cdot}_{Cr}] \gg [V^{x}_{Cr}]$, i.e. that the vanadium is tetravalent over the whole pO_2 range investigated. In this case the relation between oxide ion vacancy concentration and pO_2 can be written:

$$K = pO_2^{1/2}\,\frac{\delta(1 - x + 2\delta)^2}{(3 - \delta)(x - y - 2\delta)^2} \tag{11}$$

δ increases with decreasing pO_2 and reaches a saturation value of $(x–y)/2$ where the divalent dopant is fully ionically compensated [2]. This is illustrated in Fig. 1, where also the variation of the concentration of Cr(IV) $(=x–y–2\delta)$ with pO_2 (cf. Eq. (8)) is shown.

Results

Oxygen stoichiometry

The isothermal oxygen deficiency calculated from the thermogravimetry data are shown in Fig. 2 as function of pO_2 for 800, 900 and 1000°C. The curves on Fig. 2 represent the best fit of the experimental data with the described defect

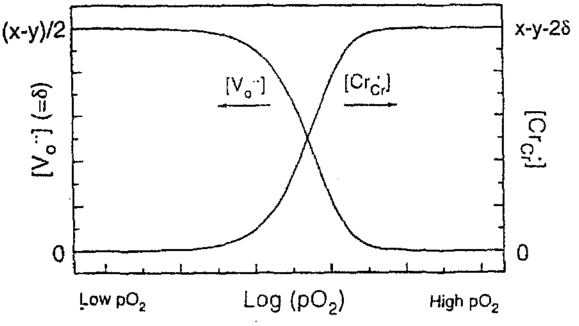

Fig. 1 Schematic presentation of the pO_2 dependence of the oxygen deficiency, δ (=$[V_o^{\cdot\cdot}]$) and [Cr$^{\cdot}$] predicted by the defect model. x and y represent the divalent A-site and tetravalent B-site dopant concentration, respectively

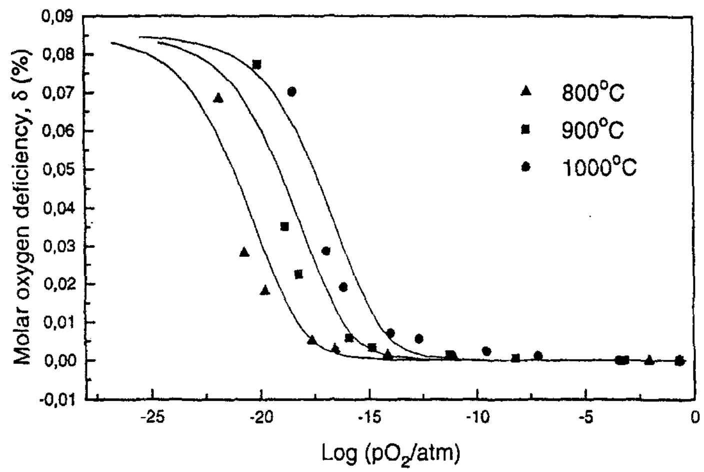

Fig. 2 Oxygen deficiency, δ, as function of pO_2. Values are calculated from isothermal thermogravimetry measurements. The solid curves represent best fit of the defect chemistry model (fitted using Eq. (11))

chemistry model. Some discrepancy is observed between the fitted curves and the experimental data. The slope in the lower part of the logpO_2 range is significantly steeper for the experimental data than predicted by the defect model, indicating a non-ideal behaviour, i.e. the formation of vacancies becomes easier with increasing δ presumably due to defect association.

An Arrhenius plot of the K-values determined from the best fit of the defect model is shown in Fig. 3 (fitted using Eq. (11), solid lines in Fig. 2). From the slope of the curve the enthalpy (ΔH^0) of formation of an oxygen vacancy can be calculated:

$$\ln K = -\Delta G^0/RT = -\frac{\Delta H^0}{RT} + \frac{\Delta S^0}{R} \qquad (12)$$

The values obtained in the present study are listed in Table 2 together with values reported in literature for other similar materials. The value of the enthalpy change is slightly lower than those observed for other similar materials. The ΔG^0 values calculated at 1000°C are also listed in Table 2. The free energy of oxygen vacancy formation is larger for the investigated material than for the purely Sr-doped material studied by Mizusaki *et al.* [2]. This agrees with the observation from Fig. 4, where the onset of the expansion for the vanadium containing material is seen to occur at a lower $p\mathrm{O}_2$ than for the LSC [8].

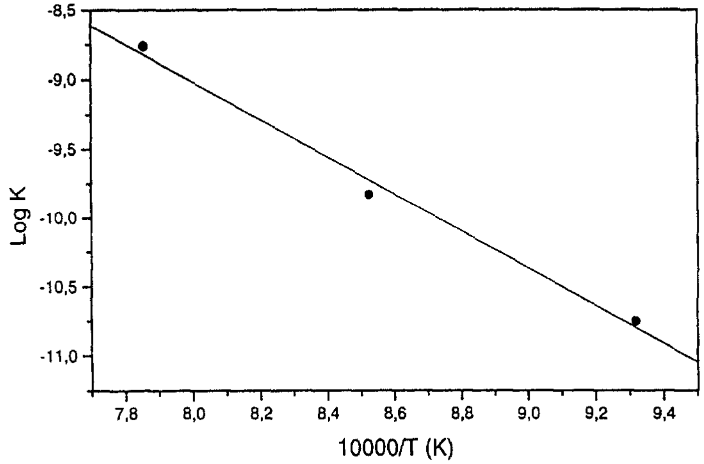

Fig. 3 Arrhenius plot showing log$K$ *vs.* temperature. K values were obtained from the best fit of the defect model (Fig. 2). ΔH^0 is determined from the slope of the line

Table 2 ΔH^0 values from present study and literature. ΔG^0 values calculated at 1000°C are given for comparison

	Dopant	x	ΔH^0/ kJ mol^{-1}	ΔG^0 1000°C/ kJ mol^{-1}
Present study	Sr/V	20/3	241+/–20	215+/–3
Yasuda [17]	Sr/Ni	20/5	289.5	170
Mizusaki [2]	Sr	20	271.7	162
Flandermeyer [4]	Mg	2–10	272+/–16	170

Measured linear expansion

The measured isothermal expansions given in percentage of sample length are plotted as function of $p\mathrm{O}_2$ at three different temperatures in Fig. 4. The onset of the expansion occurs at increasing $p\mathrm{O}_2$ with increasing temperature. For a $p\mathrm{O}_2$ level of $10^{-16.2}$ atm, which is the most reducing condition expected in a SOFC operated on steam reformed methane (at 1000°C) the expansion is approximately 0.085%. Solid and open symbols represent, respectively, experimental data from the present study

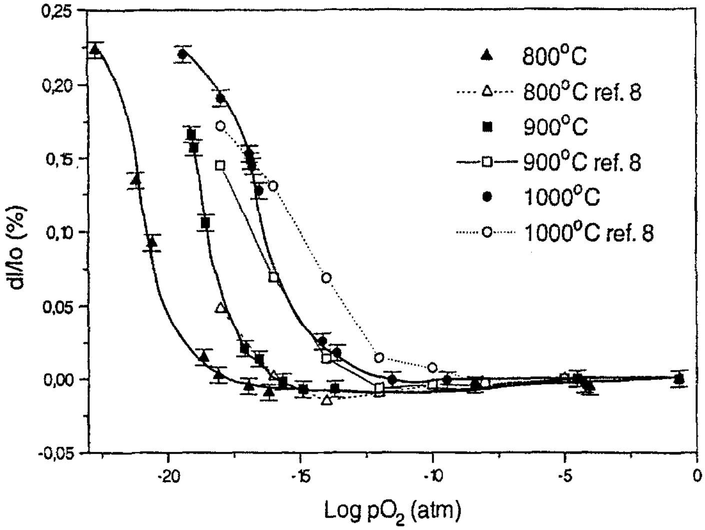

Fig. 4 Isothermal linear expansion as function of pO_2 measured by dilatometry. Solid and open symbols represent data from this work and from [8], respectively. The solid lines are drawn as guides to the eye

and expansion data for $La_{0.8}Sr_{0.2}CrO_3$ reported by Armstrong *et al.* [8]. There are significant differences in the expansion curves between the two data sets. The expansion for the samples from [8] initiates at higher pO_2 and the curves are less steep than found in the present study. At 1000°C a beginning saturation at low pO_2 is observed in both data sets. The discrepancy in expansion between the two data sets can at least partly be connected to the presence of tetravalent vanadium that initially lowers the concentration of Cr(IV) (c.f. Eq. (8)). It is known from the literature that the expansion onset moves to lower pO_2 when the A-site dopant concentration is decreasing [8]. The change in onset also agrees with the mentioned differences in free energy of oxygen vacancy formation where the higher values for the vanadium containing material suggest a later onset.

Armstrong *et al.* [8] made comparisons of isothermal expansion data with Srilomsak *et al.* [6] and Schäffer *et al.* [7] for Ca- or Sr-doped samples with various degrees of doping. Good agreement was found in the studies of Armstrong and Schäffer for the Sr-doped compositions, whereas the results for the Ca-doped compositions differed significantly. A common feature for both data sets (present work and [8]) is an initial contraction before the expansion onset. The magnitude of the contraction is most pronounced at low temperature. The mechanism that causes the contraction is not understood at present.

The expansion measured with a fixed inlet gas composition was found to be virtually independent of temperature. This is illustrated in Fig. 5, which shows the expansions measured at various temperatures for three different inlet gas compositions. For a given pO_2 the expansion will decrease with temperature. However, a

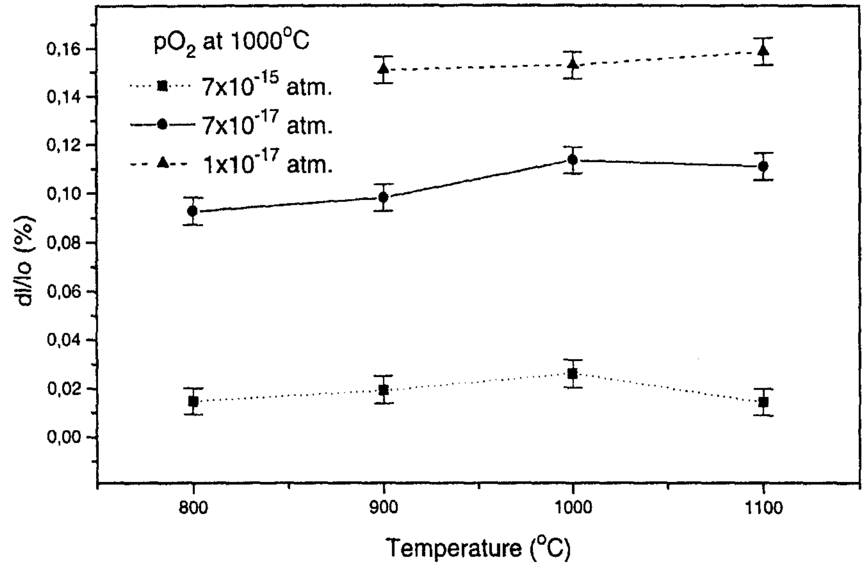

Fig. 5 Temperature dependence of the linear expansion for different gas mixtures. The EMF values are measured *vs*. air at 1000°C

fixed H_2/CO_2 ratio in the inlet gas defines a decreasing pO_2 with decreasing temperature due to change in gas equilibrium. For the investigated material the two effects almost outbalance. For practical purposes this implies that a lowering of the temperature of operation in an SOFC from 1000 to 800°C, with a fixed inlet gas composition, does not significantly decrease the magnitude of the interconnect expansion and the associated mechanical problems.

Discussion

Cause of expansion

The observed expansion is caused by the changes in the defect structure in the material with varying pO_2. At low pO_2 Cr(IV) is reduced to the larger Cr(III)-ion and oxygen ion vacancies are introduced in the lattice. The observation of an expansion indicates that effectively the volume of $2\mathrm{Cr}_{\mathrm{Cr}}^{x}+V_{\mathrm{o}}^{\cdot\cdot}$ exceeds that of $2\mathrm{Cr}_{\mathrm{Cr}}^{\cdot}+\mathrm{O}_{\mathrm{o}}^{x}$. The strong correlation between δ and expansion is illustrated in Fig. 6, where the measured expansion is plotted *vs*. the measured δ. It should be noted that δ expresses not only the vacancy concentration but also the concentration of initial Cr(IV) that has been reduced to Cr(III) at a given pO_2 (cf. Fig. 1). Initially (for δ up to 0.005–0.01) oxygen is lost without resulting in an expansion. For larger δ the sample expands with increasing δ.

It is worthwhile to speculate whether it is the oxygen ion vacancies or the increased average size of the B-site ion, or the two effects in common, that causes the

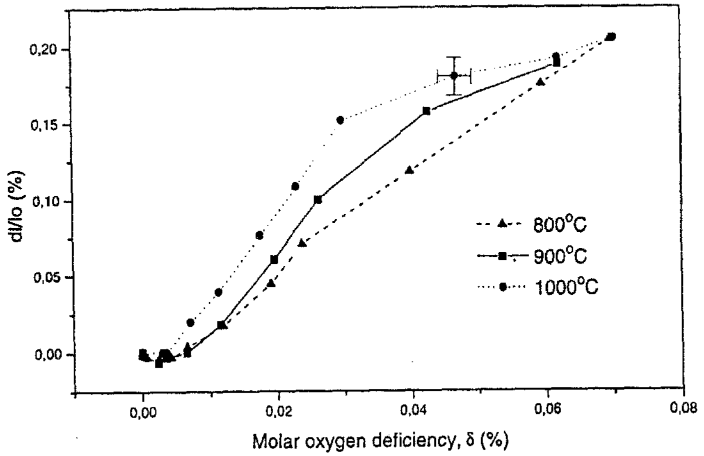

Fig. 6 Relation between isothermal linear expansion, dl/l_0, and measured molar oxygen deficiency, δ. The error bars shown for one data point represents an upper bound. It is based on the difference between a linear interpolation between data points and a fit going through all the data points (c.f. bold curves in Fig. 4)

expansion. Khattak and Cox have determined the volume of the unit cell for the $La_{1-x}Sr_xCrO_3$ system for x varying between 0 and 1 [5]. They found a linear decrease in unit cell volume with increased Sr content. The average size of the A-site ion in the lattice increases upon the substitution, as Sr(II) is larger than La(III), whereas the average size of the B-site ion decreases as part of the Cr(III) is oxidized to Cr(IV) (cf. Table 1). The observation of a net volume decrease indicates that the size-change of the B-site ion is the more dominating of the two effects. Khattak and Cox have further estimated the unit cell volume of fully reduced $La_{1-x}Sr_xCrO_{3-x/2}$. They found that the unit cell volume of $La_{1-x}Sr_xCrO_{3-x/2}$ is slightly smaller than that of $LaCrO_3$ and that it is decreasing with increasing Sr concentration. Recalling that the valence state of Cr is the same in the two cases and that Sr is larger than La, this strongly indicates that effectively the oxide vacancies decrease the volume. In other words; it is the change in average B-site ion radius upon reduction that is the major cause of the expansion. The direct effect of the oxide vacancies is smaller and probably they add negatively to the volume.

Comparison with expansion data for other dopants

The behaviour of Ca-, Sr- and Mg-doped lanthanum chromite is compared in Figs 7 and 8, where measured expansions are plotted against calculated oxygen deficiencies. In addition to the data of the present study expansion data were obtained from [8] for the case of Ca- and Sr-doping and from [15, 21] for the case of Mg-doping. The δ values for the literature data were calculated from the equivalent equilibrium equations using K-values from the literature [2, 4, 10, 17]. The δ values for this study were calculated using Eq. 11. Plotting the expansion as a function of δ the curves measured at 800, 900 and 1000°C fall very close, indicating that the main cause of the difference in the behaviour at different temperatures (cf. Fig. 4) is the temperature dependence of reaction (1). When plotted against δ, the difference between the experimental data of the present work and those of [8] is also much less than when considered as a function of pO_2, illustrating that the major cause of the difference is the difference in the value of the equilibrium constant of reaction (1). Because of the lack of experimental δ values for other materials than the one studied here, the comparison between the different materials is based on calculated δ values. The difference between the curves in Figs 6 and 7 reflects the inadequacy of the simple defect model in representing the experimental TG-data.

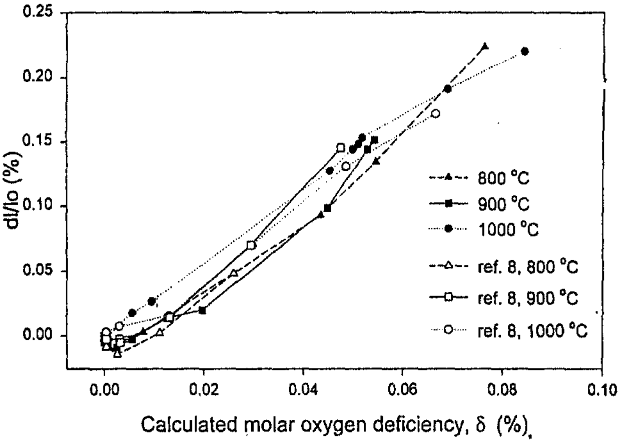

Fig. 7 Relation between measured isothermal expansion, dl/l_0, and calculated molar oxygen deficiency, δ, at three different temperatures. The data from Ref. [8] are for a 20% Sr-doped material

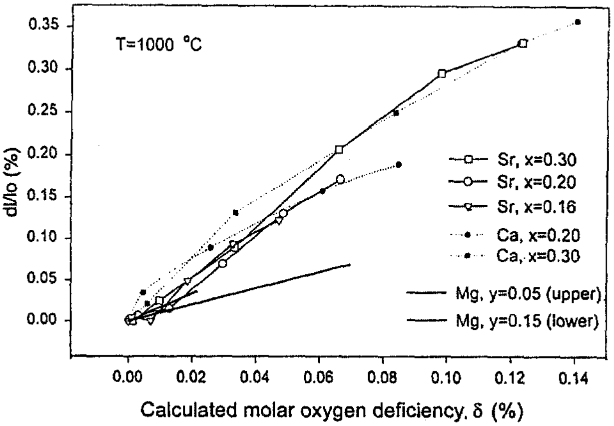

Fig. 8 Relation between measured isothermal (1000°C) expansion, dl/l_0, and calculated molar oxygen deficiency, δ, for three different dopants

The expansion behaviour of Ca- Sr- and Mg-doped lanthanum chromite measured at 1000°C is compared in Fig. 8 for various degrees of doping. The Ca- and Sr-doped samples behave very similarly at high δ, i.e. they show approximately the same expansion at a given δ. The difference observed at low and intermediate δ may in part reflect that when calculating δ, non-ideality was taken into account in the Sr-doped case [2] but not in the case of Ca-doping.

A significant difference can be seen between the A- and B-site doped compositions (Ca/Sr and Mg respectively). The Mg-doped sample expands less than half of the expansion for Sr- or Ca-doped for a given oxygen deficiency. By structural considerations it can be argued that the presence of the relative large Mg ion (0.72 Å) on the Cr(III) B-site expands the oxygen octahedra, and thereby widens the crystal structure. Therefore the material is less sensitive to the increase in ionic size during the reduction of Cr(IV) to Cr(III). This is consistent with the previously discussed observations that the unit cell volume is sensitive to the average size of the B-site ion, and the oxygen vacancies are of less importance. Evidently from Figs 7 and 8 the vanadium does not have the same stabilizing effect as the Mg (for a given δ the two 20% Sr-doped materials exhibit similar expansions). We ascribe this to the fact that V(IV) is smaller than Cr(III), i.e. it is too small to result in significant initial expansion of the oxygen octahedra that may decrease the sensitivity towards the change in average B-site ion size associated with the Cr(IV)/Cr(III) reduction.

Comparing the behaviour of the A-site doped materials with different degrees of doping, a tendency of decreasing expansion with decreasing dopant concentration is observed (at high δ). For the Mg-doped case the opposite is observed in accordance with the suggestion of the stabilizing effect of the Mg-ion on the B-site.

Tests of interconnect plates made from 20% Sr-doped lanthanum chromite in experimental SOFC stacks have revealed mechanical failure of the interconnect plates due to the dimensional instability of the material [12, 16]. More stable interconnect materials are thus required. From the above comparison between the effects of V- and Mg-doping it is anticipated that co-doping with B-site ions having ionic radii larger than that of Cr(III) may decrease the isothermal expansion. In favour of this hypothesis is a recent study [8] on the effects of adding various B-site dopants to an A-site Ca-doped composition. The results showed a decrease in isothermal expansion for several different B-site dopants, and there seem to be a good correlation between ionic size of B-site dopant and the magnitude of the isothermal expansion.

Tailoring an interconnect material for SOFC is based on a compromise where conflicting requirements are balanced: low volume expansion on reduction, high electronic conductivity, and linear thermal expansion match with other SOFC components. In the preceding discussion it has been pointed out that the volume expansion at low pO_2 primarily is caused by the reduction of Cr(IV) to Cr(III). Since the initial concentration of Cr(IV) equals the dopant concentration, a decrease in dopant concentration will decrease the volume expansion. However, the other requirements are to a certain extent favoured by an increase in dopant concentration. To increase the electronic conductivity acceptor doping on the A-site is preferable. Since the charge carriers are electron holes associated with Cr(IV) the conductivity is directly related to the A-site dopant concentration [17]. Divalent B-site doping (like Mg(II)) will also increase the Cr(IV) concentration but it will also decrease the total Cr-concentration, and thereby lower the conductivity compared to A-site doping. A match in thermal expansion coefficient between the interconnector and the other stack components, primarily the electrolyte, can be achieved by adjusting the dopant type and its concentration. An increase in TEC with increased dopant concentration and ionic radius has been reported [6, 18, 19].

Conclusion

The experimental data for $(La_{0.8}Sr_{0.2})(Cr_{0.97}V_{0.03})O_3$ showed some deviation from the defect model at low pO_2, and a comparison of expansion data with literature data showed that vanadium seems to have an influence on the isothermal expansion due to change in defect chemistry. A correlation between oxygen deficiency and expansion is demonstrated and it is argued that the expansion is caused by the volume change associated with the reduction of Cr(IV) to Cr(III). Comparison of the volume change reported in literature for different A- and B-site dopants suggests that co-doping on the B-site with ions larger than Cr(III) will expand the lattice, and thereby accommodate some of the volume change caused by the Cr(IV) to Cr(III) reduction.

* * *

This work was supported by the Danish Energy Agency and ELSAM under the DK-SOFC programme. Dr. T. R. Armstrong, The Pacific Northwest Laboratory is thanked for valuable discussions.

References

1 N. Q. Minh, J. Am. Ceram. Soc., 76 (1993) 563.
2 J. Mizusaki, S. Yamauchi, K. Fueki and A. Ishikawa, Solid State Ionics, 12 (1984) 119.
3 H. U. Anderson, J. H. Kuo and D. M. Sparlin, Proc. of 1st Int. Symp. on SOFC. Ed. S. C. Singhal, PV 89-11, Electrochemical Soc., Pennington, NJ, 1989, p. 111.
4 B. K. Flandermeyer, M. M. Nasrallah, A. K. Agarwal and H. U. Anderson, J. Am. Ceram. Soc., 67 (1984) 195.
5 C. P. Khattak and D. E. Cox, ANL-77-21 (1977) 160.
6 S. Srilomsak, D. P. Shilling and H. U. Anderson, Proc. of 1st Int. Symp. on SOFC. Ed. S. C. Singhal, PV 89-11, Electrochemical Soc., Pennington, NJ, 1989, p. 129.
7 W. Schäffer and R. Schmidberger, In: High Tech. Ceramics, Ed. P. Vincenzini, Elsevier 1987, p. 1737.
8 T. R. Armstrong, J. W. Stevenson and P. E. Raney, J. Electrochem. Soc., 143 (1996) 2919.
9 B. K. Flandermeyer, M. M. Nasrallah, D. M. Sparlin and H. U. Anderson, High Temperature Sci., 20 (1985) 259.
10 I. Yasuda and T. Hikita, J. Electrochem. Soc., 140 (1993) 1699.
11 S. W. Paulik and T. R. Armstrong, In: Proc. of the 2nd European Fuel Cell Forum, Ed. B. Thorstensen, ISBN 3-922 148-19-O. 1996, p. 547.
12 P. V. Hendriksen, J. D. Carter and M. Mogensen, In: Proceedings of 4th Int. Symp. on SOFC. Ed. M. Dokiya et al. PV 95-11, Electrochemical Soc., Pennington, NJ, 1995, p. 934.

13 N. Christiansen and P. Gordes, In Proc. 2nd International Symposium on Solid Oxide Fuel Cells, Rep. EUR 13546 EN, Commision of the European Communities, Brussels, Belgium, 1991, p. 495.
14 J. D. Carter, DK Patent 930943 A, Aug. 1993. pending.
15 H. U. Anderson, High temperature ceramics for interconnectors. Presented at: Conference on materials science issues relating to high temperature fuel cells at University of California-San Diego, 1994.
16 I. Yasuda and M. Hishinuma, In: Proc. of 4th Int. Symp. on SOFC. Ed. M. Dokiya et al. PV 95–11, Electrochemical Soc., Pennington, NJ, 1995, p. 924.
17 I. Yasuda and M. Hishinuma, Solid State Ionics, 80 (1995) 141.
18 N. Sakai, T. Kawada, H. Yokokawa and Dokiya, Solid State Ionics, 40/41 (1990) 394.
19 P. H. Larsen, C. Bagger, M. Mogensen and J. G. Larsen, In: Proc. of 4th Int. Symp. on SOFC. Ed. M. Dokiya et al. PV 95–11, Electrochemical Soc., Pennington, NJ, 1995, p. 69.
20 R. D. Shannon, Acta Cryst., A32 (1976) 751.
21 S. Srilomsak, Master thesis, University of Missori-Rolla, T5356, 1986.